

Supplemental material

JCB

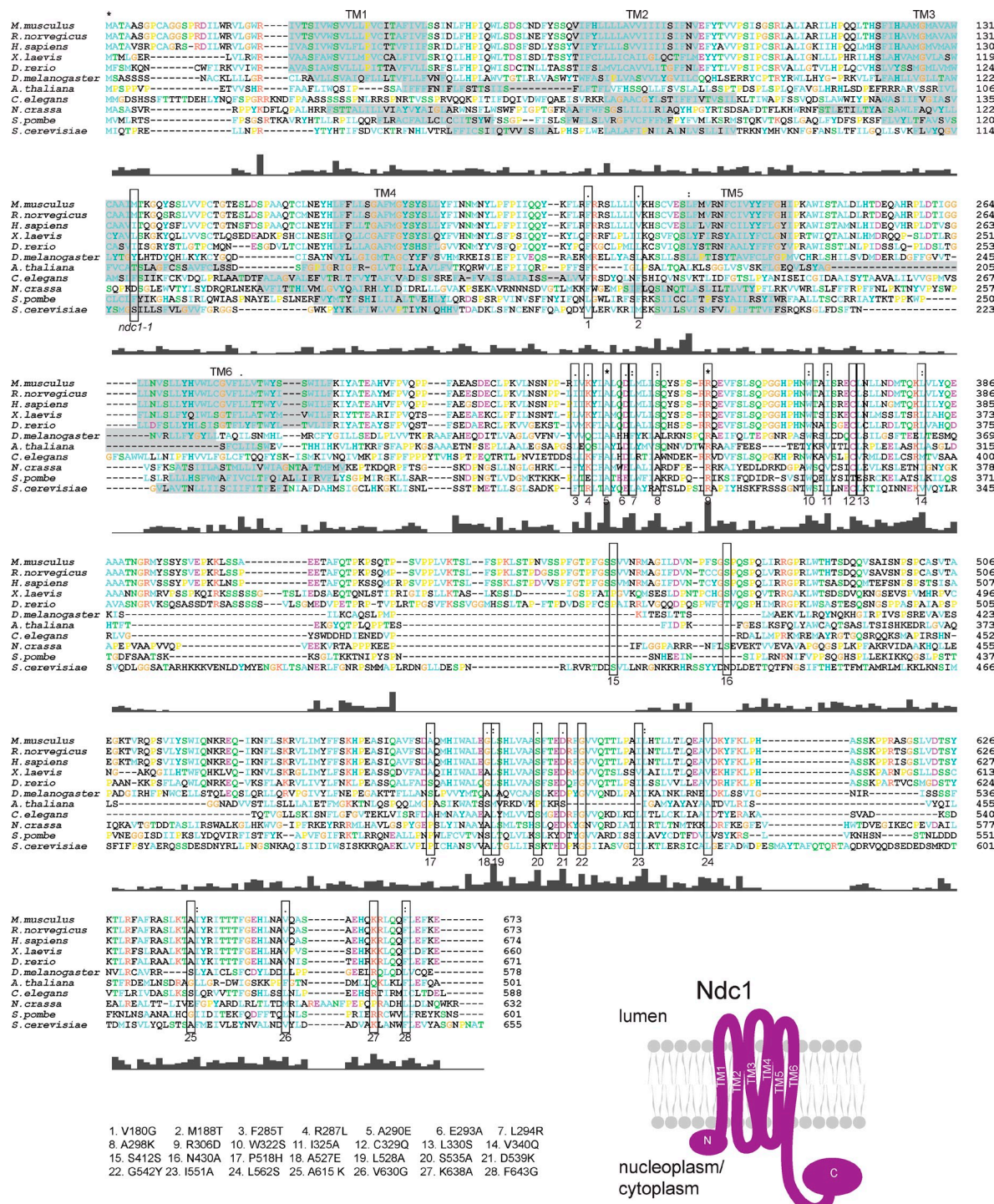
Chen et al., <http://www.jcb.org/cgi/content/full/jcb.201307043/DC1>

Figure S1. Alignment of NDC1. Ndc1 protein sequences from *Homo sapiens*, *Mus musculus*, *Rattus norvegicus*, *Xenopus laevis*, *Danio rerio*, *Drosophila melanogaster*, *Arabidopsis thaliana*, *Caenorhabditis elegans*, *Neurospora crassa*, *Schizosaccharomyces pombe*, and *Saccharomyces cerevisiae* were aligned using Clustal-W and displayed using Clustal-X. The six transmembrane domains (predicted by TMPRED software) and the positions of the 28 conserved amino acids analyzed in this study are indicated. Previous deletion analysis found that residues 368–466 in *S. cerevisiae* Ndc1 are nonessential, but all other deletions were inviable (Lau et al., 2004).

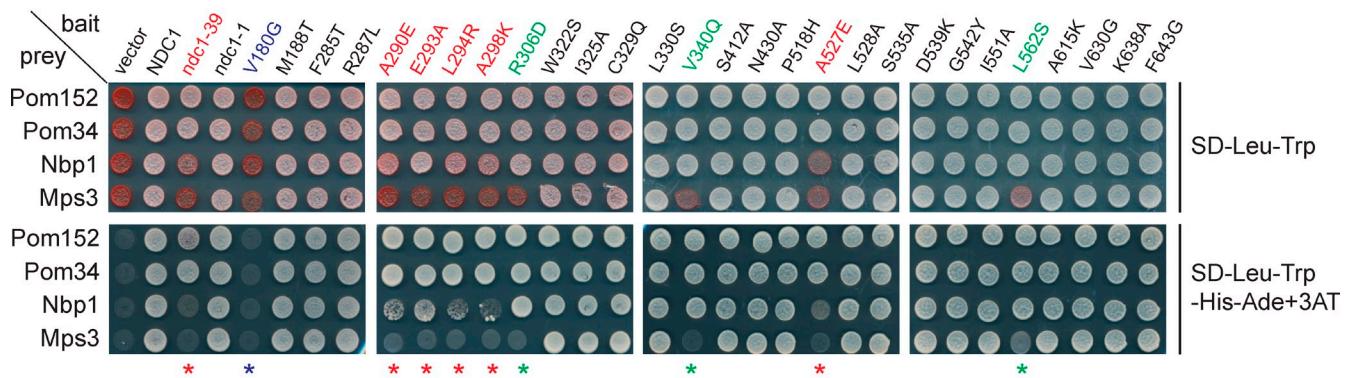
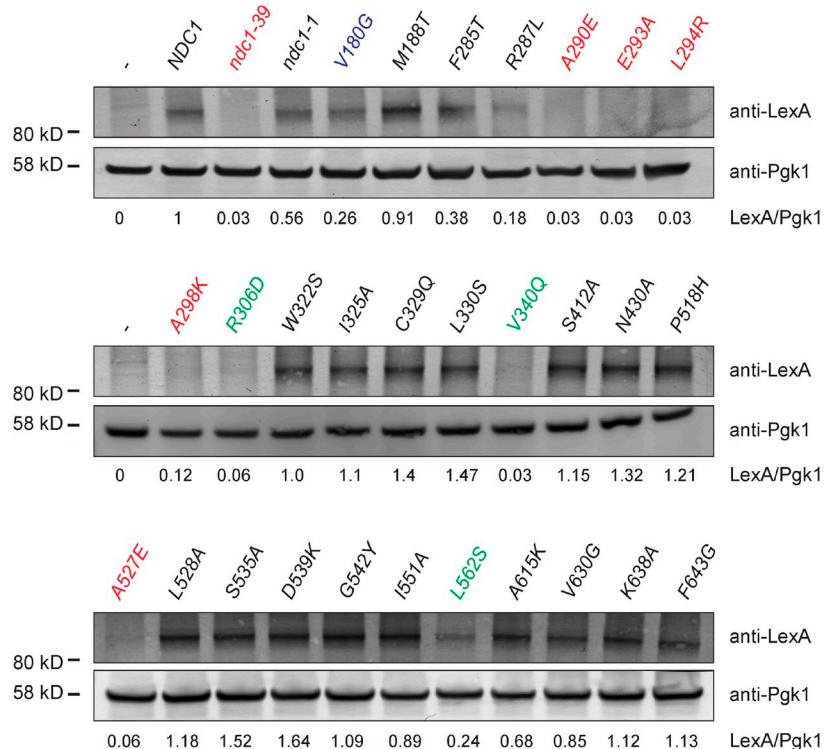
A**B**

Figure S2. MYTH analysis of *ndc1* alleles. (A) Prey plasmids containing *POM152*, *POM34*, *NBP1*, or *MPS3* were tested in combination with bait plasmids containing no insert (vector), wild-type *NDC1*, or point mutations in *NDC1* as indicated (see Fig. S1). *ndc1-1* (S119N) and *ndc1-39* (T14M, F218V, L288M, E293G, M457T, and F643L) were also characterized (Winey et al., 1993; Lau et al., 2004). The presence of both bait and prey plasmids was detected on SD-Leu-Trp media, and activation of the reporters in MYTH was assayed on SD-Leu-Trp-His-Ade plus 3-AT, which reduces background by selecting for robust expression of *HIS3*. Plates were incubated for 3 d at 30°C and then placed at 4°C overnight. Asterisks/colors indicate mutants that are described in the text and summarized in Table 1. Blue is used for the allele that is unable to bind to Pom34, Pom152, Nbp1, and Mps3; red is used for alleles that are unable to bind Nbp1 and Mps3 but bind to Pom152 and Pom34; green is used for alleles that are unable to/weakly bind to Mps3 but bind to Nbp1, Pom152, and Pom34. Although *ndc1-1* mutants have a defect in SPB duplication at 11–16°C (Winey et al., 1993), the *ndc1-1* bait was able to interact with all tested preys. Because the MYTH system does not work at low temperatures (not depicted), we were unable to test interactions at the nonpermissive temperature for this allele. (B) Expression of the baits in whole-cell extracts was analyzed by Western blotting using anti-LexA antibodies. Pgk1 served as a loading control and allowed for normalization of the levels of the baits. The strain containing an empty vector (−) was assigned a value of 0, whereas the strain containing wild-type *Ndc1* was given a value of 1. The high background of the LexA antibody made quantification difficult. For mutant alleles examined in greater detail, the addition of GFP to the baits resulted in better detection both biochemically and cytologically (see Fig. 1 F; not depicted).

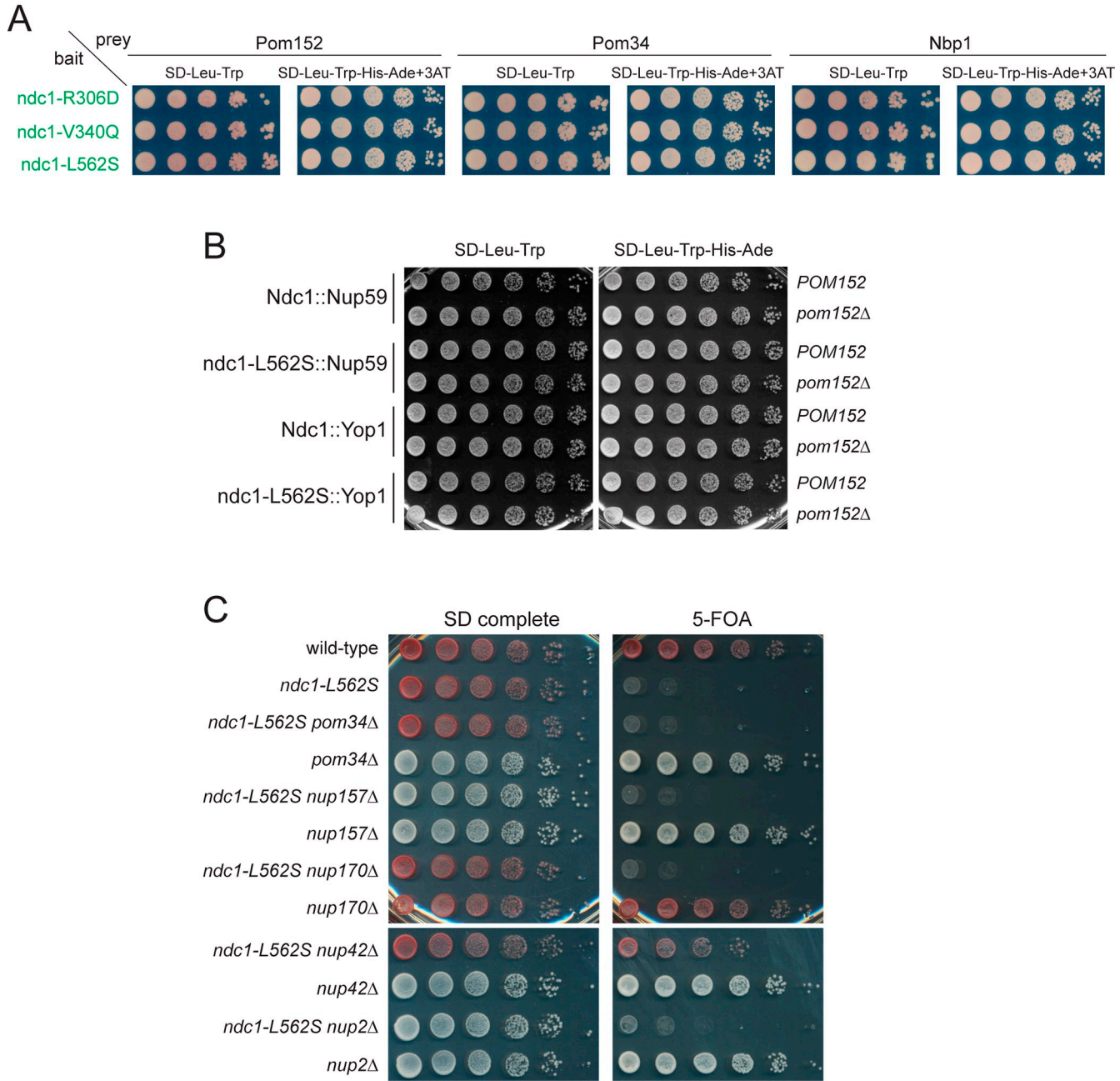


Figure S3. Relationship between *ndc1* mutants and other nucleoporins. (A) Bait and prey plasmids producing the indicated protein were tested for interaction in the MYTH strain (SLJ5572). 10-fold serial dilutions of cells were spotted onto SD-Leu-Trp and SD-Leu-Trp-His-Ade+3-AT plates that were incubated for 3 d at 30°C and then placed at 4°C overnight. The Ndc1 wild-type control is shown in Fig. 1 E. (B) Prey plasmids producing the indicated protein (Nup59 or Yop1) and bait plasmids containing *NDC1* or *ndc1-L562S* were introduced into wild-type cells used for MYTH (SLJ5572) or a version containing a deletion of *POM152* (SLJ6066). 10-fold serial dilutions of cells were spotted onto SD-Leu-Trp and SD-Leu-Trp-His-Ade and plates were incubated for 2 d at 30°C. (C) *ndc1-L562S pURA3-NDC1* was introduced into strains containing the indicated deletions, and growth of the double mutants and the single mutant parents was tested by plating 10-fold serial dilutions of cells on SD complete or 5-FOA. Plates were incubated for 3 d at 23°C.

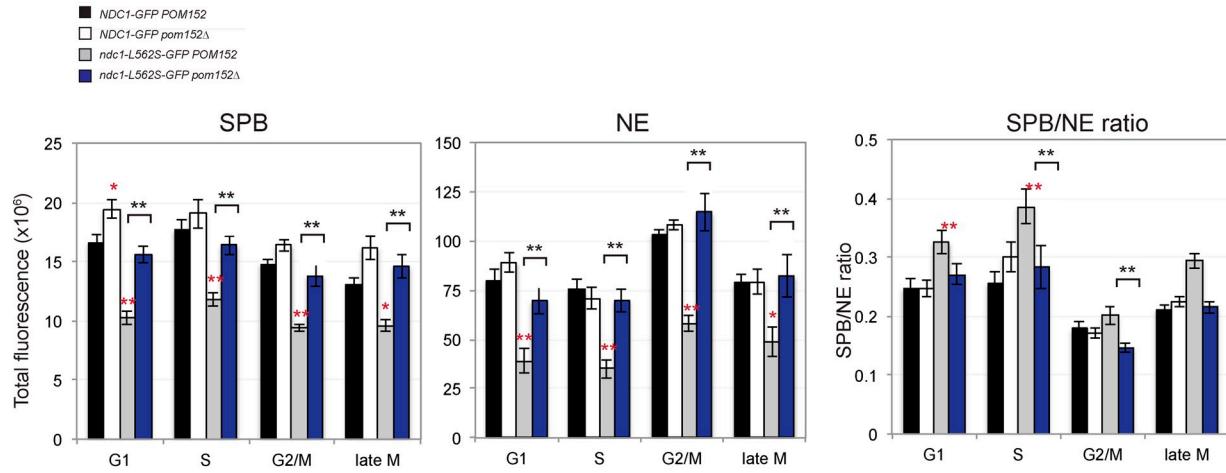


Figure S4. Levels of *ndc1-L562S* at the SPB and NE. Images from Fig. 5 A were broken down into G1, S, G2/M, and late M phases of the cell cycle using bud size, SPB number, and distance between SPBs as a marker for cell cycle position. G1 cells were defined as unbudded cells that contain a single SPB. S-phase cells were defined as cells with a small bud and a single SPB. G2/M cells had a medium to large bud and two SPBs that were separated by less than 2 μ m. Large-budded cells that contained two SPBs separated by greater than 2 μ m were defined at late M phase. The average total fluorescence intensity at the SPB and the NE is shown as well as the ratio of SPB to NE intensity. Error bars depict the SEM. Red and black single ($P < 10^{-2}$) and double asterisks ($P < 10^{-4}$) show statistically significant values compared with wild-type and the *ndc1-L562S*, respectively, using the Student's *t* test.

Table S1. Yeast strains

Strain name	Relevant genotype	Experiment
SLJ771	MAT α ADE2 lys2Δ	Fig. 1 B
SLJ6881	MAT α ndc1::NDC1-GFP-HYGMX ADE2+	Fig. 1, B and C
SLJ7484	MAT α his3Δ200 trp1-901 leu2-3, 112 ade2 LYS2::(lexAop)4-HIS3 ura3::(lexAop)8-lacZ ade2::(lexAop)8-ADE2 GAL4 ADE2+ pBT3-STE-NDC1-GFP	Fig. 1, B and C
SLJ7848	MAT α leu2::GAL-NDC1-GFP-LEU2; ADE2; lys2Δ	Fig. 1, B and C
SLJ5572	MAT α his3Δ200 trp1-901 leu2-3, 112 ade2 LYS2::(lexAop)4-HIS3 ura3::(lexAop)8-lacZ ade2::(lexAop)8-ADE2 GAL4	Figs. 1, D and E; 4, B-D; 6 A; S2; S3, A and B; Tables 1 and 2
SLJ7483	MAT α his3Δ200 trp1-901 leu2-3, 112 ade2 LYS2::(lexAop)4-HIS3 ura3::(lexAop)8-lacZ ade2::(lexAop)8-ADE2 GAL4 ADE2+	Fig. 1 F
SLJ6064	MAT α ndc1Δ::KANMX pURA3-NDC1	Figs. 2 A and 3 A
SLJ6166	MAT α ndc1Δ::KANMX::NDC1-TRP1-KANMX pURA3-NDC1	Figs. 2, A-D, 3 A, 4 E, and Tables 1 and 2
SLJ6170	MAT α ndc1Δ::KANMX::ndc1-A290E-TRP1-KANMX pURA3-NDC1	Fig. 2, A-G, Fig. 4 E, and Table 1
SLJ6167	MAT α ndc1Δ::KANMX::ndc1-39-TRP1-KANMX pURA3-NDC1	Fig. 2, A, B, and E, Table 2
SLJ6176	MAT α ndc1Δ::KANMX::ndc1-A527E-TRP1-KANMX pURA3-NDC1	Fig. 2, A and B, Table 1
SLJ6168	MAT α ndc1Δ::KANMX::ndc1-1-TRP1-KANMX pURA3-NDC1	Fig. 2 A
SLJ6169	MAT α ndc1Δ::KANMX::ndc1-V180G-TRP1-KANMX pURA3-NDC1	Fig. 2 A, Table 1
SLJ6171	MAT α ndc1Δ::KANMX::ndc1-E293A-TRP1-KANMX pURA3-NDC1	Fig. 2 A, Table 1
SLJ6172	MAT α ndc1Δ::KANMX::ndc1-L294R-TRP1-KANMX pURA3-NDC1	Fig. 2 A, Table 1
SLJ6173	MAT α ndc1Δ::KANMX::ndc1-A298K-TRP1-KANMX pURA3-NDC1	Fig. 2 A, Table 1
SLJ6321	MAT α pom152Δ::NATMX ndc1Δ::KANMX::ndc1-V180G-TRP1-KANMX pURA3-NDC1	Table 1
SLJ6322	MAT α pom152Δ::NATMX ndc1Δ::KANMX::ndc1-E293A-TRP1-KANMX pURA3-NDC1	Table 1
SLJ6323	MAT α pom152Δ::NATMX ndc1Δ::KANMX::ndc1-L294R-TRP1-KANMX pURA3-NDC1	Table 1
SLJ6324	MAT α pom152Δ::NATMX ndc1Δ::KANMX::ndc1-A298K-TRP1-KANMX pURA3-NDC1	Table 1
SLJ6325	MAT α pom152Δ::NATMX ndc1Δ::KANMX::ndc1-V340Q-TRP1-KANMX pURA3-NDC1	Table 1
SLJ6795	MAT α NUP49-mCherry-HYGMX ADE2+	Fig. 2 H
SLJ7486	MAT α ndc1Δ::KANMX::ndc1-A290E-TRP1-KANMX NUP49-mCherry-HYGMX ADE2+	Fig. 2 H
SLJ6174	MAT α ndc1Δ::KANMX::ndc1-R306D-TRP1-KANMX pURA3-NDC1	Fig. 3 A, Table 1
SLJ6175	MAT α ndc1Δ::KANMX::ndc1-V340Q-TRP1-KANMX pURA3-NDC1	Fig. 3 A, Table 1
SLJ6179	MAT α pom152Δ::NATMX ndc1Δ::KANMX::ndc1-A290E-TRP1-KANMX pURA3-NDC1	Fig. 4 E, Table 1
SLJ6178	MAT α pom152Δ::NATMX ndc1Δ::KANMX::ndc1-TRP1-KANMX pURA3-NDC1	Fig. 4 E, Tables 1 and 2
SLJ6180	MAT α pom152Δ::NATMX ndc1Δ::KANMX::ndc1-L562S-TRP1-KANMX pURA3-NDC1	Fig. 4 E, Tables 1 and 2
SLJ6181	MAT α pom152Δ::NATMX ndc1Δ::KANMX::ndc1-39-TRP1-KANMX pURA3-NDC1	Fig. 4 E, Table 2
SLJ001	MAT α	Fig. 3, A and B; Fig. S3 C
SLJ6177	MAT α ndc1Δ::KANMX::ndc1-L562S-TRP1-KANMX pURA3-NDC1	Figs. 3 A, 4 E, 5 D, S3 C, and Table 2
SLJ6367	MAT α ndc1Δ::KANMX::NDC1-3HA-HIS3MX-TRP1-KANMX leu2::GAL1-NDC1-GFP-LEU2	Fig. 3, B, C, and F
SLJ6369	MAT α ndc1Δ::KANMX::ndc1-L562S-3HA-HIS3MX-TRP1-KANMX leu2::GAL1-NDC1-GFP-LEU2 pURA3-NDC1	Fig. 3, B, C, and G-I
SLJ6847	MAT α ndc1Δ::KANMX::ndc1-L562S-3HA-His3MX-TRP1-KANMX leu2::GAL1-NDC1-GFP-LEU2 SPC42-mCherry-HYGMX GFP-TUB1-NATMX pURA3-NDC1	Fig. 3, D and E
SLJ6848	MAT α ndc1Δ::KANMX::NDC1-3HA-HIS3MX-TRP1-KANMX leu2::GAL1-NDC1-GFP-LEU2 SPC42-mCherry-HYGMX GFP-TUB1-NATMX	Fig. 3, D and E
SLJ6822	MAT α ndc1Δ::KANMX::NDC1-3HA-HIS3MX-TRP1-KANMX leu2::GAL1-NDC1-GFP-LEU2 NUP49-mCherry-HYGMX ADE2+	Fig. 3 J
SLJ6823	MAT α ndc1Δ::KANMX::ndc1-L562S-3HA-HIS3MX-TRP1-KANMX leu2::GAL1-NDC1-GFP-LEU2 NUP49-mCherry-HYGMX pURA3-NDC1	Fig. 3 J
SLJ6066	MAT α pom152Δ::KANMX his3Δ200 trp1-901 leu2-3, 112 ade2 LYS2::(lexAop)4-HIS3 ura3::(lexAop)8-lacZ ade2::(lexAop)8-ADE2 GAL4 ADE2+	Figs. 4 D, 6 A, S3 B, and Table 2
SLJ6288	MAT α ndc1Δ::KANMX::NDC1-GFP-HIS3MX-TRP1-KANMX SPC42-mCherry-URA3 pLEU2-NDC1	Fig. 5, A-C, Fig. S4
SLJ6588	MAT α pom152Δ::NATMX ndc1Δ::KANMX::NDC1-GFP-HIS3MX-TRP1-KANMX SPC42-mCherry-URA3 pLEU2-NDC1	Fig. 5, A-C, Fig. S4
SLJ6638	MAT α ndc1Δ::KANMX::ndc1-L562S-GFP-HIS3MX-TRP1-KANMX SPC42-mCherry-HYGMX pLEU2-NDC1	Fig. 5, A-C, Fig. S4
SLJ6734	MAT α pom152Δ::NATMX ndc1Δ::KANMX::ndc1-L562S-GFP-HIS3MX-TRP1-KANMX SPC42-mCherry-HYGMX pLEU2-NDC1	Fig. 5, A-C, Fig. S4
SLJ910	MAT α mps3-1 pURA3-MPS3	Fig. 5 E
SLJ7436	MAT α MPS3-YFP-HIS3MX NDC1-mTurq-URA3MX	Fig. 6, B-F

Table S1. Yeast strains (Continued)

Strain name	Relevant genotype	Experiment
SLJ7438	<i>MATα pom152Δ::HYGMX MPS3-YFP-HIS3MX NDC1-mTurq-URA3MX</i>	Fig. 6, B–F
SLJ7835	<i>MATα NUP49-YFP-NATMX ndc1Δ::KANMX::NDC1-mTurq-HIS3MX-TRP1-KANMX ADE2+</i>	Fig. 6, G and H
SLJ7836	<i>MATα pom152Δ::HYGB NUP49-YFP-NATMX ndc1Δ::KANMX::NDC1-mTurq-HIS3MX-TRP1-KANMX ADE2+</i>	Fig. 6, G and H
SLJ6833	<i>MATα pom34Δ::HYGB ndc1Δ::KANMX::ndc1-L562S pURA3-NDC1 LYS+</i>	Fig. S3 C
SLJ6729	<i>MATα pom34Δ::HYGMX</i>	Fig. S3 C
SLJ6773	<i>MATα nup157Δ::HYGMX</i>	Fig. S3 C
SLJ6769	<i>MATα nup170Δ::HYGMX</i>	Fig. S3 C
SLJ6772	<i>MATα nup42Δ::HYGMX</i>	Fig. S3 C
SLJ6770	<i>MATα nup2Δ::HYGMX</i>	Fig. S3 C
SLJ6935	<i>MATα nup157Δ::HYGMX ndc1Δ::KANMX::ndc1-L562S-TRP1-KANMX pURA3-NDC1</i>	Fig. S3 C
SLJ6936	<i>MATα nup170Δ::HYGMX ndc1Δ::KANMX::ndc1-L562S-TRP1-KANMX pURA3-NDC1</i>	Fig. S3 C
SLJ6934	<i>MATα nup42Δ::HYGMX ndc1Δ::KANMX::ndc1-L562S-TRP1-KANMX pURA3-NDC1</i>	Fig. S3 C
SLJ6933	<i>MATα nup2Δ::HYGMX ndc1Δ::KANMX::ndc1-L562S-TRP1-KANMX pURA3-NDC1</i>	Fig. S3 C

References

- Lau, C.K., T.H. Giddings Jr., and M. Winey. 2004. A novel allele of *Saccharomyces cerevisiae NDC1* reveals a potential role for the spindle pole body component Ndc1p in nuclear pore assembly. *Eukaryot. Cell.* 3:447–458. <http://dx.doi.org/10.1128/EC.3.2.447-458.2004>
- Winey, M., M.A. Hoyt, C. Chan, L. Goetsch, D. Botstein, and B. Byers. 1993. NDC1: a nuclear periphery component required for yeast spindle pole body duplication. *J. Cell Biol.* 122:743–751. <http://dx.doi.org/10.1083/jcb.122.4.743>